

# INVESTIGATION OF MODIFIED SCREEN-PRINTING AL PASTES FOR LOCAL BACK SURFACE FIELD FORMATION

Vichai Meemongkolkiat<sup>1</sup>, Kenta Nakayashiki<sup>1</sup>, Dong Seop Kim<sup>1</sup>, Steve Kim<sup>2</sup>, Aziz Shaikh<sup>2</sup>, Armin Kuebelbeck<sup>3</sup>, Werner Stockum<sup>3</sup>, and Ajeet Rohatgi<sup>1</sup>

<sup>1</sup>School of Electrical and Computer Engineering, Georgia Institute of Technology, Atlanta, GA 30332, U.S.A.

<sup>2</sup>Ferro Corporation, 1395 Aspen Way, Vista, CA 92083, U.S.A.

<sup>3</sup>Merck KGaA Darmstadt, Frankfurter Str. 250, 64293 Darmstadt, Germany

## ABSTRACT

This paper reports on a low-cost screen-printing process to form a self-aligned local back surface field (LBSF) through dielectric rear surface passivation. The process involved formation of local openings through a dielectric ( $\text{SiN}_x$  or stacked  $\text{SiO}_2/\text{SiN}_x$ ) prior to full area Al screen-printing and a rapid firing. Conventional Al paste with glass frit degraded the  $\text{SiN}_x$  surface passivation quality because of glass frit induced pinholes and etching of  $\text{SiN}_x$  layer, and led to very thin LBSF regions. The same process with a fritless Al paste maintained the passivation quality of the  $\text{SiN}_x$ , but did not provide an acceptably thick and uniform LBSF. Al pastes containing appropriate additives gave better LBSF because of the formation of a thicker and more uniform Al-BSF region. However, they exhibited somewhat lower internal back surface reflectance (<90%) compared to conventional Al paste on  $\text{SiN}_x$ . More insight on these competing effects is provided by fabrication and analysis of complete solar cells.

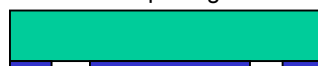
## INTRODUCTION

In the crystalline Si solar cell industry, screen-printing of Al followed by Al-Si alloying at moderate temperature (700-800°C) is widely used to form a full area Al-back surface field (Al-BSF), which provides a good ohmic contact and reasonable passivation on the back side of the cell. However, to improve the energy conversion efficiency, a process scheme that incorporates a higher quality back surface passivation and provides good optical confinement is needed, especially if the cell thickness is reduced. Surface passivation of Si by dielectric layers (e.g. thermally grown  $\text{SiO}_2$  or plasma-enhanced chemical vapor deposited (PECVD)  $\text{SiN}_x$ ) has been proven to be quite effective [1]. Additionally, it is known that deposition of metal on a dielectric layer can provide exceptional internal reflection [2,3], which is highly desirable for optical confinement. However, the main hindrance preventing the use of this structure lies in the development of a cost-effective process to make electrical contact through these dielectric layers with a good ohmic contact, without deteriorating the passivation quality. A simple process scheme to achieve such a structure is developed in this study. The process, outlined in Fig. 1, involves formation of local

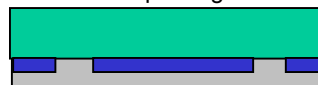
1. Dielectric passivation of the rear surface



2. Formation of local opening in the rear dielectric



3. Full area Al screen-printing



4. Short time annealing

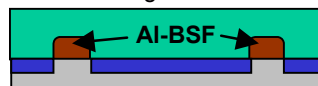


**Fig 1.** Schematic of simple process for dielectric back passivation with LBSF.

openings through the dielectric prior to full area Al screen-printing followed by a rapid annealing. A similar structure for local back contact has been proposed and reported in [4,5]. With dielectric layer as a mask, local contact is only made through the openings, while high quality back passivation and back reflection are maintained elsewhere. Furthermore, the use of screen-printed Al provides a self-aligned local-BSF (LBSF) underneath the contact. This LBSF is crucial for obtaining a good ohmic contact especially on high resistivity substrates (>1  $\Omega\text{-cm}$ ) and minimizing the effect of high recombination at the metal interface.

The objective of this paper is to provide guidelines for choosing the appropriate Al-paste to achieve such a structure. The dielectric layers used in this paper are a low frequency PECVD  $\text{SiN}_x$  and a stack of thin thermal oxide and PECVD  $\text{SiN}_x$ . In this study, two modified Al alloyed pastes (paste A and paste B) were developed by adding appropriate additives to fritless Al paste. Consequently, four different Al pastes were investigated: 1) *fritted* Al paste (regular Al paste with the glass frit commercially used for full area Al-BSF structure), 2) *fritless* Al paste, 3) paste A with additive, and 4) paste B with different amount of additive. These four pastes were first analyzed on the basis of three criteria: 1) maintenance of dielectric passivation

quality, 2) internal back surface reflection and 3) formation of an LBSF. Finally, LBSF cells with screen-printed contacts were fabricated and analyzed with light IV measurement and long wavelength light beam-induced current (LBIC) response.

## EXPERIMENTAL

The wafers included in this study were all  $\sim 2.5 \Omega\text{-cm}$  B-doped float zone (FZ) Si. The surface passivation quality of dielectric layers after Al firing was studied by first growing a thin thermal oxide ( $\sim 100 \text{ \AA}$ ) at  $875^\circ\text{C}$  in a conventional tube furnace. Then a  $\text{SiN}_x$  film with a thickness of  $\sim 650 \text{ \AA}$  was deposited on the rear side on top of the  $\text{SiO}_2$  layer in a low-frequency direct PECVD reactor. Subsequently, the four Al pastes were screen-printed on the rear side of each sample followed by  $\sim 750^\circ\text{C}/\sim 3\text{s}$  annealing in a belt furnace. Additionally,  $\text{SiN}_x$  coated samples without Al were included in the annealing as a reference. All samples with Al were then placed in  $\text{HCl}:\text{H}_2\text{O}_2:\text{H}_2\text{O}$  (1:1:2 by volume) to remove the Al layer. Finally, the effective lifetime was measured by the photoconductance decay method at an excess carrier concentration of  $2 \times 10^{14} \text{ cm}^{-3}$ .

The internal back surface reflection was studied by depositing  $\sim 1000 \text{ \AA}$  of  $\text{SiN}_x$  film on both sides of FZ Si samples. Then, the four Al pastes were screen-printed on the rear side of each sample. Additionally, one sample with  $\text{SiN}_x$  on the front only and fritted Al on the back was prepared as a reference. All samples were annealed in the belt furnace using the same condition as discussed above. Finally, the total reflectance was measured on the front side of the structures.

To study the local BSF formation, test structures were prepared according to the process scheme shown in Fig. 1. The openings were formed by screen-printing of SolarEtech paste from Merck KGaA (an HF-free paste containing special  $\text{PO}_4^{3-}$  complex for  $\text{SiO}_2$  and/or  $\text{SiN}_x$  selective etching) with a  $125 \times 125 \mu\text{m}^2$  square pattern. The etching paste was annealed to initiate the etching reaction and then rinsed in DI water to remove etching residue. The four Al paste were then screen-printed on the backside and annealed in the belt furnace. Cross-sections of all samples were prepared for SEM analysis by sectioning through the vias, polishing, and etching to delineate the  $p\text{-}p^+$  region [6]. This allowed examination of the LBSF under the contacts.

Finally,  $4 \text{ cm}^2$  LBSF solar cells with screen-printed contacts were fabricated. First, a  $\sim 45 \Omega/\text{sq}$  emitter was formed by  $\text{POCl}_3$  diffusion followed by back side Si etch to remove the  $n^+$  layer from the backside. Then, a thin thermal oxide ( $\sim 100 \text{ \AA}$ ) was grown followed by deposition of  $\sim 650 \text{ \AA}$  of  $\text{SiN}_x$  on both sides. The local openings on the backside were formed using the SolarEtech paste as described above. All samples were then subjected to full-area Al screen-printing on the backside using the four Al pastes, followed by Ag gridline printing on the front. The samples were then co-fired in the belt furnace. The cells were analyzed using light IV measurement and LBIC response.

## RESULTS AND DISCUSSIONS

### Effect of annealing on the passivation quality of $\text{SiO}_2/\text{SiN}_x$ with printed Al on top

A summary of effective lifetime measured on  $\text{SiO}_2/\text{SiN}_x$  coated wafers after annealing with Al followed by removal of Al is shown in Fig. 2. The results show that the FZ wafer with  $\text{SiO}_2/\text{SiN}_x$  passivation had an effective lifetime of  $400 \mu\text{s}$  and all three fritless Al pastes on  $\text{SiO}_2/\text{SiN}_x$  maintained the effective lifetime at  $400\text{--}500 \mu\text{s}$  after firing. This result demonstrates that the presence of the additive in the Al paste did not degrade the dielectric passivation quality. On the other hand, the use of fritted Al paste significantly lowered the effective lifetime  $130 \mu\text{s}$ . This is attributed to the glass frit reaction with  $\text{SiN}_x$  layer, resulting in the degradation of  $\text{SiN}_x$  passivation quality.

### Effect of Al paste composition on the internal back surface reflection

Figure 3 shows the total reflectance in the long wavelength for different Al pastes on  $1000 \text{ \AA}$  of  $\text{SiN}_x$ . The results show that all of the metal-dielectric systems provided higher escape reflectance compared to full area Al-BSF structure, indicating superior internal back reflection. However, the presence of the additive in Al (pastes A and B) seems to lower the reflectivity of the metal-dielectric system. Following the method used in [2], the back surface reflectance for each structure were extracted: 94%, 93%, 89%, 88% for fritted Al, fritless Al, paste A and paste B on dielectric, respectively. On the other hand, A much lower back surface reflectance of 62% was obtained on regular Al-BSF structure.

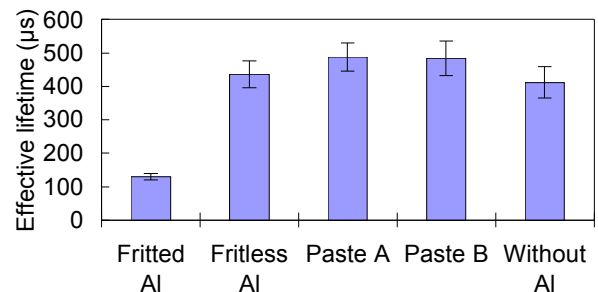


**Fig 2.** Effective lifetime of  $\text{SiO}_2/\text{SiN}_x$  passivated samples after annealing with different Al pastes on top.

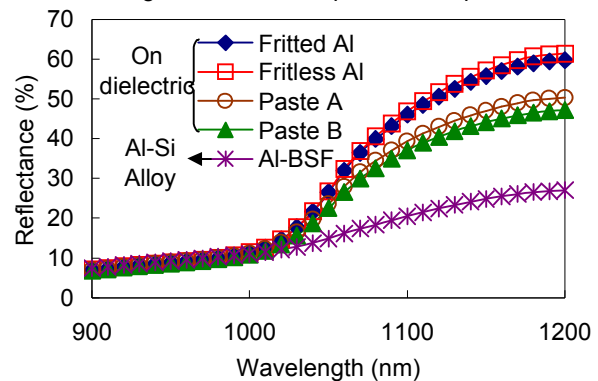


**Fig 3.** Total reflectance in the long wavelength range for different back structures.

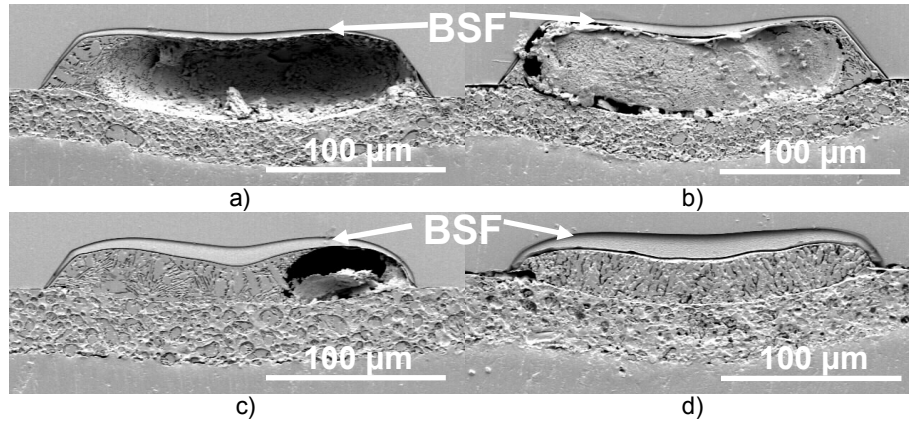
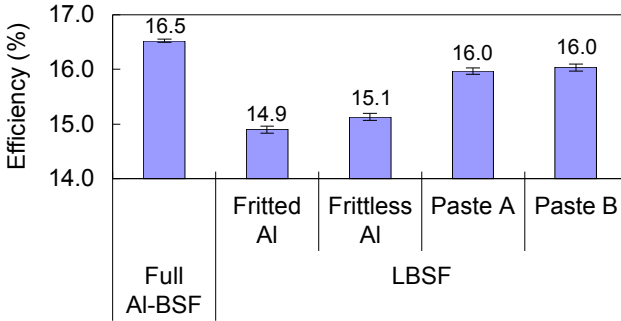


**Fig 4.** Cross-sectional SEM micrographs of LBSF for different Al pastes: a) fritted Al, b) fritless Al, c) paste A, and d) paste B.

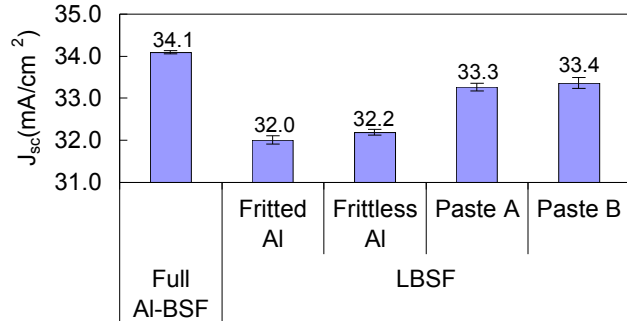
#### Study of local BSF formation with different Al pastes

SEM micrographs of the local Al-BSF regions formed with the four pastes are shown in Fig. 4. The BSF region under the Al contact is quite thin (up to only 6  $\mu\text{m}$ ) when the fritted Al and fritless Al pastes without the additive are used. Our calculations show that a 6  $\mu\text{m}$  thick Al-BSF can lead to a BSRV of 640  $\text{cm/s}$  on 1  $\Omega\text{-cm}$  wafers. On the other hand, pastes A and B with appropriate additives provided a BSF as thick as 13.5  $\mu\text{m}$  thick that is much more uniform. This BSF thickness can lead to a BSRV of 290  $\text{cm/s}$  on 1  $\Omega\text{-cm}$  wafers.

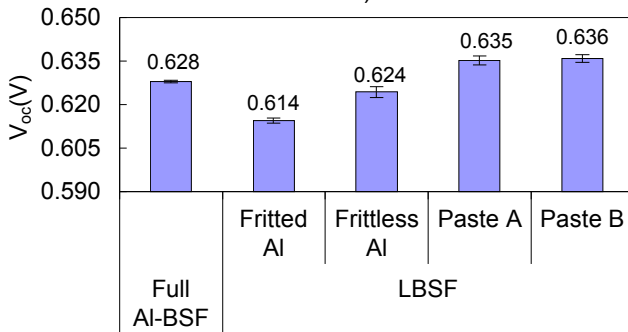
#### Effect of Al paste composition on the performance of LBSF solar cells



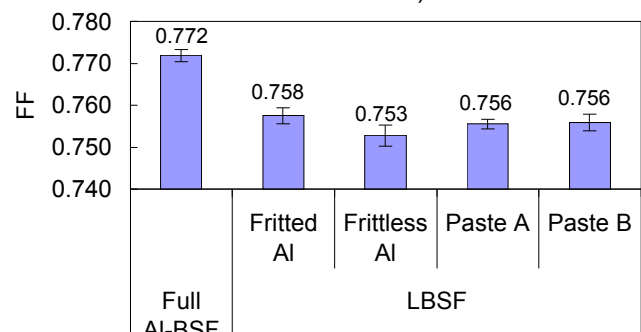
a)



b)



c)



d)

**Fig. 5.** (a) Efficiency, (b)  $J_{sc}$ , (c)  $V_{oc}$ , and (d) FF of screen-printed solar cells with different structures.

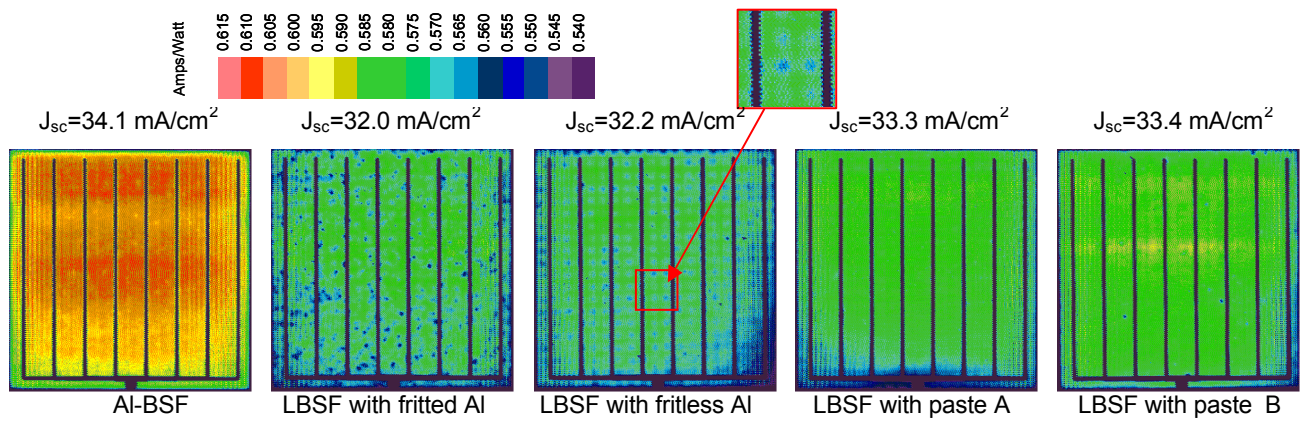


**Fig. 6.** Long wavelength LBIC responses of screen-printed solar cells with different structures.  $J_{sc}$  for each structure from Fig. 5b was included for comparison.

The spatial uniformity of the back surface passivation in full area Al-BSF and LBSF cells was evaluated using LBIC. The long wavelength (980 nm) LBIC responses for five cells (including a full area Al-BSF cell) are shown in Fig. 6. The LBIC responses are in very good agreement with the  $J_{sc}$  values in Fig. 5b. This implies that the trend of  $J_{sc}$  shown in Fig. 5b is mainly a result of the difference in BSRV (as bulk lifetime is acceptably high in these FZ samples). The LBSF cell with fritted Al shows very poor response, which is attributed to the degradation of  $\text{SiN}_x$  after annealing caused by frit- $\text{SiN}_x$  reaction and the poor LBSF. The LBSF cell with fritless Al has better response in between the point contact; however, it clearly shows lower response at the point contact which is a result of poor LBSF as shown in Fig. 4. On the other hand, both the LBSF cells with modified Al pastes show a uniform response at the point contacts and in the region in between them. However, the overall responses are lower for these cells compared to the regular full area Al-BSF. This is most likely attributed to the parasitic shunting of inversion layers in these cells, resulting in higher effective back surface recombination especially for  $J_{sc}$  condition. Under  $V_{oc}$  condition, the shunting effect is less pronounced, that is why the  $V_{oc}$  of LBSF cells with additive is higher (Fig. 5c).

## CONCLUSIONS

This paper demonstrates a low-cost screen-printing process to form a self-aligned local back surface field through a  $\text{SiO}_2/\text{SiN}$  dielectric stack. The process yields an excellent surface recombination value of 35 cm/s due to the high-quality dielectric stack and a high BSR in regions between the rear Al point contacts. The modified Al pastes also form a uniform  $>10 \mu\text{m}$ -thick LBSF under the contacts without deteriorating the passivation quality of the dielectric. The use of these modified Al pastes results in a significant improvement in the LBSF solar cell performance as compared to conventional Al pastes. The  $V_{oc}$  of the LBSF cells using modified paste was 7-8 mV higher than that in conventional full area Al cells. However, the cell efficiency for LBSF cells was lower due to losses in  $J_{sc}$

and FF, which are attributed to the parasitic shunting between the back contact and the inversion layer.

## REFERENCES

- [1] J. Schmidt, M. Kerr, and A. Cuevas, "Surface Passivation of Silicon Solar Cells Using Plasma-Enhanced Chemical-Vapor-Deposited  $\text{SiN}$  Films and Thin Thermal  $\text{SiO}_2/\text{Plasma SiN}$  Stacks", *Semicond. Sci. Technol.*, **16**, 2001, pp. 164-170.
- [2] A. Ristow, M. Hilali, A. Ebong, and A. Rohatgi, "Screen-Printed Back Surface Reflector for Light Trapping in Crystalline Silicon Solar Cells", *Seventeenth EU-PVSEC*, 2001, pp. 1335-1338.
- [3] O. Schultz, M. Hofmann, S.W. Glunz, and G.P. Willeke, "Silicon Oxide / Silicon Nitride Stack System for 20% Efficient Silicon Solar Cells", *Thirty-first IEEE PVSC*, 2005, pp. 872-876.
- [4] G. Agostinelli, P. Choulat, H.F.W. Dekkers, S. De Wolf, and G. Beaucarne, "Screen Printed Large Area Crystalline Silicon Solar Cells on Thin Substrates", *Twentieth EU-PVSC*, 2005, pp. 647-650.
- [5] G. Agostinelli, J. Szlufcick, P. Choulat, and G. Beaucarne, "Local Contact Structures for Industrial Perc-Type Solar Cells", *Twentieth EU-PVSC*, 2005, pp. 942-945.
- [6] W.R. Runyan, *Semiconductor Measurements and Instrumentation*, (McGraw-Hill, New York, 1975).
- [7] S.R. Wenham et al., "Rear Surface Effects in High Efficiency Silicon Solar Cells", *First WCPEC*, 1994, pp. 1278-1282.
- [8] S. Dauwe, L. Mittelstädt, A. Metz, and R. Hezel, "Experimental Evidence of Parasitic Shunting in Silicon Nitride Rear Surface Passivated Solar Cells", *Prog. Photovolt: Res. Appl.* **10**, 2002, pp. 271-278.